JOURNAL OF PHYSIOLOGY AND PHARMACOLOGY 2019, 70, 1, 153-165
www.jpp.krakow.pl | DOI: 10.26402/jpp.2019.1.15

G. GORCZYCA[1], K. WARTALSKI[1], Z. TABAROWSKI[2], M. DUDA[1]

EFFECTS OF VINCLOZOLIN EXPOSURE ON THE EXPRESSION AND ACTIVITY OF SIRT1 AND SIRT6 IN THE PORCINE OVARY

[1]Department of Endocrinology, Institute of Zoology and Biomedical Research, Jagiellonian University, Cracow, Poland;
[2]Department of Experimental Hematology, Institute of Zoology and Biomedical Research, Jagiellonian University, Cracow, Poland

Within the mammalian reproductive system sirtuin 1 and 6 (SIRT1, SIRT6) are considered to contribute to steroid hormone signaling and control of reproductive physiology. Therefore, the specific question is whether and how a commonly used dicarboximide fungicide with antiandrogenic activity, vinclozolin (Vnz) alters SIRT1 and SIRT6 expression and whether both investigated sirtuins positively affect survival of the follicles after vinclozolin exposure. Immunocytochemistry and immunohistochemistry were performed to localize SIRT1 and SIRT6 expression in cultured granulosa cells (GCs; 48 hours) and whole ovarian follicles (24 hours) after treatment with two androgens, testosterone (T; 10^{-7} M) and dihydrotestosterone (DHT; 10^{-7} M), and an antiandrogen, Vnz (1.4×10^{-5} M), separately and in combinations. Granulosal and follicular mRNA and protein expression of both sirtuins was also investigated by real-time PCR and Western blot. In addition, their concentration and activity was studied by immunoenzymatic and fluorescence assays. Our observations: (1) demonstrate the presence of both investigated sirtuins in ovarian cells, (2) show their potential involvement in the control of follicular atresia because of increased SIRT1/SIRT6 expression and SIRT1 activity after exposure to Vnz, (3) represent the first data on the interrelationships between sirtuins and androgens in porcine ovarian cells. Based on these findings and our previous results we can conclude, that SIRT1 and SIRT6 do not exert the protective effects in ovarian follicles after vinclozolin exposure. These novel data on the role of SIRT1/SIRT6 in porcine ovarian follicles shows that in the presence of the investigated fungicide, sirtuins are upregulated, which can induce apoptosis of follicular cells. Furthermore the androgen receptor sensitivity to ligands, especially environmental ones (for example: vinclozolin) might be directly linked with the mechanism of action of both investigated sirtuins in the porcine ovary, which requires further investigation.

Key words: *nicotinamide adenine dinucleotide-dependent deacetylase, granulosa cells, ovarian follicle, vinclozolin, sirtuin*

INTRODUCTION

Silent information regulator 2 (Sir2) is a nicotinamide adenine dinucleotide (NAD)+-dependent deacetylase that connects metabolism with longevity in yeast and worms. Mammals contain 7 homologs of yeast Sir2: sirtuins 1 through 7 (SIRT 1-7), which are highly conserved proteins and expressed in multiple tissues (1). They show distinct subcellular localizations: SIRT1, 6 and 7 are found in the nucleus, SIRT2 is in the cytoplasm, while SIRT3, 4 and 5 in the mitochondria (2). Sirtuins are implicated in many physiological processes such as regulation of energy metabolism, steroid hormone receptors dynamics, apoptosis and cell cycle regulation (3-5). They are also working as stress adaptors to oxidative, genotoxic and metabolic stress (6). SIRT1 and SIRT6, being of our special interest, play important roles in a variety of biological processes such as stress and cytokine responses, proliferation and differentiation, apoptosis and metabolism (7, 8). These two sirtuins have been shown to protect the genome from mutations that can drive tumorigenesis. Regarding the female reproductive system, the expression and activity of SIRT1 has been observed in mammalian ovaries, granulosa cells, oocytes, and embryos (9-11). It was shown that continuous overexpression of SIRT1 in oocytes enhances reproductive capacity, preserves ovarian reserve and extends ovary lifespan in mice (12). It was also observed that SIRT1 has a role in porcine follicle atresia (13), granulosa cells proliferation and secretory activity (14, 15).

The mechanisms regulating recruitment, growth and development of ovarian follicles are under control of hormones, including pituitary gonadotropins, and locally produced growth factors, which are synthesized within the follicle (16, 17). Among them are androgens, steroid hormones. Numerous *in vivo* and *in vitro* animal studies, as well as clinical reports, established that androgens are crucial for normal follicular development and function (18, 19). They act *via* androgen receptors (ARs) at different stages of folliculogenesis (20). They are able to promote early follicular growth and increase the number of growing and ovulatory follicles. Androgens can also contribute to follicular atresia (21). Based on recent literature (22, 23) and our previous findings (24, 25), it is notable that

disturbed androgens action affects female fertility. In pigs, we have shown that administration of some antiandrogens led to altered follicular steroidogenesis as well as apoptosis of cultured granulosa cells (GCs) or atresia of whole follicles (26, 27).

The increasing human exposure to agents capable of inducing changes in the genetic material (mutagenic agents) is a consequence of industrial development and the adoption of certain habits within the modern society. Many of these substances, called endocrine disrupting compounds (EDCs), interact with nuclear receptors of steroid hormones and thereby can interfere with the functioning of the endocrine system. Vinclozolin (Vnz), a commonly used dicarboximide fungicide registered in the USA and Europe to prevent the decay of fruits and vegetables, belongs to EDCs. Two major ring-opened metabolites of Vnz (butenoic acid M1 and enanilide M2) were detected in rodent fluids and tissue extracts following *in vivo* exposure (28). Vnz possesses an antiandrogenic activity in mammals and fish (29, 30). Exposure to Vnz during the gonadal sex determination period in mice promotes a transgenerational increase in pregnancy abnormalities and female adult onset malformations in the reproductive organs (31, 32). Our previous studies show that Vnz reduces porcine GCs viability and proliferation while disturbing the physiological process of programmed cell death (27, 33). Thus, this environmental antiandrogen may activate non-genomic signaling pathways directly modifying the AR signaling pathway (34).

Keeping in mind the crucial role of androgens in folliculogenesis and data on the correlation between ARs and the activity of sirtuins (35-37), we hypothesize that an experimentally induced androgen availability disturbance during porcine granulosal and follicular culture affects sirtuins expression. Therefore the specific aim of the present study was to investigate the possible changes of SIRT1 and SIRT6 expression in the porcine ovary induced by exposure to a commonly used dicarboximide fungicide with an antiandrogenic activity, vinclozolin, *in vitro*. Additionally, the present study was designed to test whether SIRT1 and/or SIRT6 can compensate for the harmful effects induced by Vnz.

MATERIAL AND METHODS

Animals

Porcine ovaries were excised from Polish Landrace gilts (approximately 7 to 8 months of age and weighing 80 to 90 kg) at a local slaughterhouse and placed in sterile ice-cold phosphate-buffered saline (PBS; pH 7.4, PAA The Cell Culture Company, Piscataway, NJ, USA) containing Antibiotic/Antimycotic Solution (AAS; 5 mL/500 mL, PAA the Cell Culture Company). Ovaries were transported to the laboratory within 1 hour. Next, the experimental material was rinsed twice with sterile PBS containing antibiotics. Approximately 20 pig ovaries from 10 animals were selected for follicle isolation in each experiment. Assuming that each ovary yielded 3 – 5 follicles, the total number of follicles varied from 60 to 100. Based on our experience and knowledge, using criteria described by Lin *et al.* (38) in each experiment, only healthy, small-sized follicles (2 – 4 mm in diameter) were selected for cell isolation.

Granulosa cells isolation, culture and preparation for immunocytochemical analysis

Isolation of GCs was performed according to a technique developed and modified in our laboratory (33, 39). Briefly, the cells were scraped from the follicular wall with round-tip ophthalmologic tweezers. GCs were washed a few times in sterile PBS and recovered by centrifugation (90 × g for 10 min). Erythrocytes were removed using Red Blood Cell Lysis Buffer (Sigma-Aldrich, St. Louis, MO, USA). The viability of the GCs was estimated using the trypan blue exclusion test (mean ± SD: 95 ± 2%; Sigma-Aldrich). Isolated cells were seeded in 24-well culture plates (Nunc, Kalmstrup, Denmark) at an initial number of 6 ± 10^5 cells/mL (for immunocytochemical analysis) or in 6-well culture plates (Nunc) at an initial number of 16×10^5 cells/mL (for Western blots). Each well of the 24-well plate was equipped with a round, non coated coverslip. For ELISAs, GCs were seeded in 96-well culture plates at an initial density of 5×10^4 cells/mL. GCs were cultured in DMEM/F12 medium (Sigma-Aldrich) supplemented with 10% fetal bovine serum (FBS; PAA The Cell Culture Company) and AAS in a humidified atmosphere of 95% air: 5% CO_2 at 37ºC for 24 hours to enable cell attachment to the culture plate. Afterward, culture media were changed (5% FBS) (33) and testosterone (T; 10^{-7} M; Sigma-Aldrich), dihydrotestosterone (DHT; 10^{-7} M; Sigma-Aldrich) (40, 41), or Vnz (1.4×10^{-5} M; Sigma-Aldrich) were added separately or in combinations (31). Combinations consisted of T and Vnz (T + Vnz), or DHT and Vnz (DHT + Vnz). T, one of the main ovarian sex steroids, is converted to estradiol or estrone *via* the composite action of aromatase (P450arom) (42). T can also be converted by 5α-reductase to DHT, which is thought to be a more potent androgen than T because of its higher affinity for the AR. Furthermore, DHT cannot be aromatized to estradiol (43). All the applied factors were dissolved in dimethyl sulfoxide (DMSO; Sigma-Aldrich); its final concentration in the culture medium did not exceed 0.1%. Solvent controls also included 0.1% DMSO. At this concentration, DMSO had no effect on GC morphology, proliferation or viability (trypan blue exclusion was greater than 95%), (not shown). After the next 24 h of culture, immunolocalization of sirtuins was performed. Remaining cells were collected and frozen at –70ºC for further sirtuins mRNA and protein expression analysis. All experiments were performed in quadruplicate (four wells) in five separate cultures (n = 5 independent experiments).

Follicle culture and preparation for immunohistochemical analysis

Whole follicles were isolated from porcine ovaries (n = 54, 2 – 4 mm in diameter). Since the ovarian follicles have a three-dimensional structure the maintenance such an organization during the *in vitro* culture is crucial for their proper development. Therefore, follicular cultures in 3D-system in alginate hydrogel were conducted. This method (44) was modified in our laboratory. Briefly, the fibrinogen/alginate (Sigma-Aldrich) solution was prepared by mixing 0.5% alginate solution with 50 mg/mL fibrinogen solution at a 1:1 ratio. Next, 15 µL drops of the fibrinogen/alginate mixture were pipetted onto a parafilm coated glass slide. After that one follicle was transferred into each drop with a minimal amount of culture media. 15 µL of thrombin/Ca^{2+} (Sigma-Aldrich) solution was added to each drop. After forming the gel, the alginate beads were covered with the second parafilm coated glass slide and putted upside down to the incubator for 5 minutes. After that time, beads were transferred into a 46 well culture plate containing 300 µL of DMEM/F12 medium supplemented with 10% FBS and AAS for 24 hours. Experimental cultures were performed in the presence of T (10^{-7} M; Sigma-Aldrich), DHT (10^{-7} M; Sigma-Aldrich), or Vnz (1.4×10^{-5} M; Sigma-Aldrich) separately or in combination (31). For immunohistochemical analysis, follicles (n = 3/each group) were fixed in 4% paraformaldehyde, subsequently dehydrated in an increasing gradient of ethanol, and embedded in paraplast (Sigma-Aldrich). Sections of 5 µm in thickness were mounted on slides

coated with 3-aminopropyltriethoxysilane (Sigma-Aldrich). Additionally, follicles (n = 3/each group) were collected and frozen at –70ºC for further mRNA and protein expression analysis.

Immunocytochemistry and immunohistochemistry

Immunocytochemistry and immunohistochemistry were performed using the NovoLink Polymer Detection System (Leica Biosystems Newcastle Ltd, Newcastle Upon Tyne, UK) according to the manufacturer's instructions. Cells were washed in PBS and fixed in 2% paraformaldehyde. Then, permeabilization of cell membranes was performed using 0.1% Triton X-100 (Sigma-Aldrich) in Tris-buffered saline (TBS; pH 7.4). To extinguish the activity of endogenous peroxidase, cells were treated with Peroxidase Block for 10 min. In the next step, non-specific binding sites were blocked by incubation with Protein Block in a humidity chamber for 10 min at room temperature. Next, cells were incubated with a primary antibody raised against SIRT1 or SIRT6 (polyclonal anti-rabbit SIRT1 in a 1:20 dilution, sc-15404 Santa Cruz Biotechnology, Santa Cruz, CA, USA; polyclonal anti-rabbit SIRT6 in a 1:20 dilution, LS-B5589 LifeSpan BioScience, Inc. Seattle, AWA, USA) overnight at 4ºC in a humidity chamber. After incubation, cells were rinsed a few times in TBST (TBS + 0.1% Tween 20, Sigma-Aldrich) and incubated with the Post Primary (NovoLink Polymer Detection System) for 30 min at room temperature in a humidity chamber. Then, cells were washed again in TBST and incubated with NovoLink™ Polymer for 35 min at room temperature in a humidity chamber in the dark. The reaction was visualized using 3,3'-diaminobenzidine (DAB; Sigma-Aldrich). Thereafter, cells were washed, and mounted with Shandon Immu-Mount™ media (Thermo Shandon Limited, subsidiary of Thermo Fisher Scientific, Manor Park, UK). Negative controls were performed by replacing of the primary antibody with non-immune rabbit IgG.

Follicle sections of 5 µm thickness were deparaffinized in xylene for 20 min to remove the embedding medium. The slides were rehydrated in a decreasing series of ethanol dilutions (100%, 90%, 70% and 50%). For antigen retrieval, the sections were immersed in 10 mM citrate buffer pH 6.0 or Tris-EDTA buffer (10 mM Tris and 1mM EDTA pH 9.0 containing 0.05% (v/v) Tween 20) and heated twice for 5 min each in a microwave oven (750 W). Endogenous peroxidase activity was prevented by incubation in 3% hydrogen peroxide in methanol for 30 min. After that immunohistochemistry for SIRT-1 or -6 was performed using the NovoLink Polymer Detection System (Leica Biosystems Newcastle Ltd), as it was described for immunocytochemistry. Finally, the slides were washed for 5 min in running water and dehydrated in a series of graded ethanol baths before rinsing in two xylene baths and mounting in DPX (Sigma-Aldrich). Negative controls were performed by replacing the primary antibody with a non-immune rabbit IgG.

Semi-quantitative evaluation of staining intensity

The cells and follicular sections were photographed using a Nikon Eclipse E200 microscope and Coolpix 5400 digital camera (Nikon Instruments Europe B.V., Amsterdam, The Netherlands) with the corresponding software. Immunoreactivity was estimated semi-quantitatively; image analyses were performed on each coverslip with at least 500 cells and three different sections from each examined follicle using ImageJ software (National Institutes of Health, Bethesda, MD, USA). The intensity of SIRT1 and SIRT6 staining was expressed as a relative optical density, ROD = $OD_{specimen}/OD_{background}$ = $\log(GL_{blank}/GL_{specimen})/\log(GL_{blank}/GL_{background})$, where GL is the gray level for the stained area (specimen) and unstained area (background), whereas blank is the gray level measured after the slide was removed from the light path (45).

Western blot analysis

After termination of culture, GCs were washed in sterile PBS. Then, whole protein was extracted using 0.5 mL of radioimmunoprecipitation assay buffer (RIPA; Thermo Scientific, Inc., Rockford, IL, USA) in the presence of a protease inhibitor cocktail (Sigma-Aldrich). Thereafter, cells were scraped, sonificated, and recovered by centrifugation (14,000 rpm for 15 min at 4ºC). Porcine follicles were first homogenized on ice with cold Tris/EDTA buffer (50 mM Tris and 1 mM EDTA, pH 7.4), subsequently sonificated, and centrifuged as GCs. The supernatant from samples of GCs and follicles was collected and stored at –70ºC. Protein concentrations for each sample were quantified using a NanoDrop ND2000 Spectrophotometer (Thermo Scientific, Wilmington, DE, USA). Aliquots of cellular and follicular samples containing 30 µg of protein were solubilized in a sample buffer (Bio-Rad Laboratories, GmbH, Munich, Germany) and then heated for 5 min at 99.9ºC. After denaturation, protein samples were separated through electrophoresis on a 10% SDS-polyacrylamide gel under reducing conditions according to Laemmli (46). Subsequently, separated proteins were transferred onto a nitrocellulose membrane using a wet blotter with Genie Transfer Buffer (20 mM Tris and 150 mM glycine in 20% methanol; pH 8.4) for 180 min at 250 mA. Membranes were blocked in a solution of 5% w/v not-fat dry milk in TBST (TBS × 0.1% Tween 20) overnight at 4ºC with gentle shaking. Next, membranes were incubated with a polyclonal anti-SIRT1 or anti-SIRT6 antibody at a 1:1000 dilution (for details see the immunocytochemistry and immunohistochemistry subsection) for 1.5 h at room temperature. Then, blots were washed in TBST and incubated with the secondary antibody horseradish-peroxidase (HRP) labeled goat anti-rabbit antibody at a dilution of 1:1000 (Vector Laboratories, Inc.) for 1 hour at room temperature. To control for variable amounts of protein, the membranes were stripped and reprobed with mouse monoclonal anti-β-actin antibody (dilution 1 : 3000; Sigma-Aldrich) and with horseradish peroxidase-conjugated anti-mouse IgG (dilution 1 : 3000; Bio-Rad Laboratories Inc., GmbH, München, Germany). The signals of the reaction were detected by chemiluminescence using Western Blotting Luminol Reagent (sc-2048, Santa Cruz Biotechnology, Santa Cruz, CA, USA). Membranes were visualized using the ChemiDoc XRS$^+$ System (Bio-Rad Laboratories GmbH). All bands were quantified using ImageJ software (National Institutes of Health, Bethesda, MD, USA). Molecular masses were estimated by reference to ColorBurst Electrophoresis Marker (Sigma-Aldrich). To obtain semi-quantitative results, the bands representing each data point were densitometrically scanned using IMAGE LAB 2.0 software (Bio-Rad Laboratories Inc.). Each data point was normalized against its corresponding β-actin data point. Semi-quantitative analysis was performed for three separately repeated experiments from each control and experimental groups.

RNA isolation and reverse transcription (RT)-PCR analysis

Total cellular RNA from GCs was isolated using Tri Reagent solution (Ambion, Austin, TX, USA) following the manufacturer's instructions. Total cellular RNA from incubated ovarian follicles was isolated using a NucleoSpin RNA II kit (Macherey-Nagel GmbH & Co., Duren, Germany) also according to the manufacturer's protocol. The quantity and quality of the total RNA were ascertained by measuring absorbance at 260 and 280 nm with a NanoDrop ND2000 Spectrophotometer (Thermo

Scientific, Wilmington, DE, USA). Moreover, RNA samples were electrophoresed on a 1% (wt/vol) denaturing agarose gel to verify RNA quality and stored frozen at –80º C. First-strand cDNA was prepared by RT with the use of 1 µg of total RNA, random primers, and a High-Capacity cDNA Reverse Transcription Kit (Applied Biosystems, Foster City, CA, USA) according to the manufacturer's protocol. The 20 µL total reaction volume contained random primers, dNTP mix, RNAse inhibitor, and Multi Scribe Reverse Transcriptase. RT was performed in a Veriti Thermal Cycler (Applied Biosystems) according to the following thermal profile: (1) 25ºC for 10 min, (2) 37ºC for 120 min, and (3) 85ºC for 5 min. Genomic DNA amplification contamination was checked by control experiments in which reverse transcriptase was omitted during the RT step. Samples were kept at –20ºC until further analysis.

Quantitative real-time PCR

Real-time PCR analyses were performed using TaqMan Gene Expression Master Mix and porcine-specific TaqMan Gene Expression Assay (Applied Biosystems) for SIRT1 (Ss03374091_m1) and SIRT6 (Ss03387359_u1) with an endogenous glyceraldehyde-3-phosphate dehydrogenase (GAPDH, Ss03375629_uL) control, following the manufacturer's instructions. All real-time PCR experiments were performed in duplicate (47). Amplifications were performed with a StepOne™ real-time PCR System (Applied Biosystems) according to the recommended cycling program (2 min at 50ºC, 10 min at 95ºC, 40 cycles of 15 s at 95ºC, and 1 min at 60ºC). Amplification of contaminating genomic DNA was checked by control experiments in which reverse transcriptase was omitted during the RT step. Threshold cycles (Ct values) for the expression of the investigated gene were calculated using StepOne software. All samples were normalized to GAPDH ($^{\Delta\Delta Ct}$ value). The relative expression of the genes of interest was expressed as $2^{-\Delta\Delta Ct}$ (48).

ELISA analysis

Sirtuin-1 and -6 concentrations in cell lysates was measured by commercially available ELISA kits: SIRT1 ELISA Kit (CSB-E15058h) and SIRT6 ELISA Kit (CSB-E17018h), according to the manufacturer's instructions (Cusabio Biotech CO., LTD, College Park, MD, USA). Briefly, cell lysates was plated into wells and incubated at 37ºC for 30 min. Antibody specific for SIRT1 or -6 has been pre-coated onto microplates. Standards and samples were pipetted into the wells and any SIRT1 or -6 present was bound by the immobilized antibody. After removing any unbound substances, a biotin-conjugated antibody specific for SIRT1 or -6 was added to the wells. After washing, avidin conjugated horseradish peroxidase (HRP) was added to the plates. Following a wash to remove any unbound avidin-enzyme reagent, a substrate solution was added to the wells and color developed in proportion to the amount of both sirtiuns bound in the initial step. The color development was stopped and its intensity was measured at 405 nm using an ELISA ELx808 reader (BIO-TEK Instruments, Winooski, VT, USA) Results were analyzed using KC JUNIOR software (BIO-TEK Instruments). Findings were normalized to the control and underwent logarithmic transformation. The inter- and intra-run precision had CVs of 3.0% and 3.5%, respectively.

Sirtuin 1 activity assay

For Sirt1 activity cultured GCs were assayed using SIRT1 Assay Kit (Sigma-Aldrich) according to the manufacturers' instructions, where dose dependency curve of recombinant SIRT1 activity ranges from 0 – 4890 × 10^{-2} counts/min with SIRT1 content from 1 to 120 ng, respectively. The Sirt1 Assay Kit is based on the deacetylation of a synthetic substrate by Sirt1, consisting of four amino acids with one acetylated lysine group (Arg-His-Lys-Lys(Ac)) and a fluorochrome. The substrate was incubated with samples along with NAD+ as a co-substrate. After deacetylation, the fluorochrome was specifically released only from the deacetylated substrate. Fluorescence was measured at a excitation wavelength of 360 nm and an emission wavelength of 460 nm using a microplate spectrophotometer (Infinite M200; TECAN Group, Mannedorf, Switzerland). Sirt1 deacetylation activity was expressed as a percentage of control.

Statistical analysis

Statistical analysis was performed using Statistica 10.0 software (StatSoft, Inc., Tulsa, OK, USA). For GC experiments, n = 5, and for whole follicle incubations, n = 3 (GCs were performed in quadruplicate and whole follicles were performed in triplicate). The Shapiro-Wilk test for normality and the one-way ANOVA followed by Tukey's *post hoc* test were used to assess differences between control and experimental cultures. Immunocyto-/immunohistochemistry, real-time PCR, Western blotting, ELISAs and fluorescence assays were repeated three times (in duplicate). The data were expressed as the mean ± SEM. Statistical significance was established at $*P \leq 0.05$, $**P \leq 0.01$, and $***P \leq 0.001$.

RESULTS

The effect of vinclozolin on granulosal/ovarian sirtuins localization

To identify specific cellular localization of the investigated sirtuins as well as to examine potential differences induced by androgen/antiandrogen addition, immunocyto- and immunohistochemical staining was applied.

Immunohistochemistry revealed that both investigated sirtuins were present in all performed variants of granulosal cell cultures (*Figs. 1* and *3*) as well as in cultured follicles (*Figs. 2* and *4*) obtained from control and androgen/antiandrogen supplemented cultures.

In cultured granulosa cells, the intensity of SIRT1 staining was higher in both Vnz and DHT+Vnz ($P \leq 0.001$, $P \leq 0.01$, respectively) groups compared with the control group. In detail, expression of SIRT1 was observed usually in the nucleus or in the perinuclear region of granulosa cells from control cultures and androgens-stimulated ones. Interestingly, in GCs cultured under combinations of an androgen and an antiandrogen, T + Vnz and DHT + Vnz, the signal was usually dispersed throughout the cytoplasm or sporadically assembled in the perinuclear region. It was also observed that the addition of Vnz to the culture medium, alone or simultaneously with androgens, influenced the shape and morphology of cells that appeared to be less flattened.

The intensity of SIRT6 staining was significantly higher in Vnz ($P \leq 0.01$) and DHT + Vnz ($P \leq 0.01$) groups, when compared to the control (*Fig. 3*). The staining was usually located in the nucleus or in the perinuclear region. What was interesting, in GCs cultured with DHT + Vnz, strong cytoplasmic signal was observed.

In sections of whole cultured follicles, SIRT1 immunoreactivity was observed in various cell types obtained from both control and experimental conditions (*Fig. 2*). In the GCs, SIRT1 was predominantly detected in the nuclear compartment or in the perinuclear region. Sporadically, staining was observed in

the cytoplasm. Similar situation was observed within theca cells (TCs), where SIRT1 was mainly detected in the nuclear compartment except for follicles cultured with DHT + Vnz, where strong cytoplasmic signal was observed. SIRT1 expression in GCs was consistently higher within antral granulosa layer (AGL) with a decreasing intensity towards mural layer (MGL). There was one exception - homogenous SIRT1 staining intensity was detected in follicles cultured under T influence. The intensity of SIRT1 staining was the strongest in both Vnz ($P \leq 0.01$) and DHT + Vnz ($P \leq 0.01$) supplemented groups compared with the control group.

In cultured follicles, positive signal for SIRT6 was mainly shown within the nuclei of follicular cells (*Fig. 4*). The intensity of SIRT6 staining was significantly higher in both T+Vnz ($P \leq 0.01$) and DHT + Vnz ($P \leq 0.01$) groups, when compared to the control.

The effect of vinclozolin on granulosal SIRT1 and SIRT6 protein concentration and activity

Immunodetectable SIRT1 protein was observed as a single band near the 120 kDa, while SIRT6 protein was characterized by two bands near 30 and 40 kDa, position of the SDS gel, in both granulosal (*Fig. 5*) and follicular homogenates (*Fig. 6*). Stripped immunoblots were also used for actin that served as a control for equal protein loading. The bands were analyzed densitometrically, and the data obtained for each protein were normalized against its corresponding β-actin.

Western blot analyses were performed to examine the effect of androgens/antiandrogen on SIRT1 and SIRT6 expression at protein level in porcine granulosal (*Fig. 5A'* and *5B'*) and follicular (*Fig. 6A'* and *6B'*) cultures. In granulosal cultures, the expression of SIRT1 protein was downregulated in both T + Vnz ($P \leq 0.05$) and DHT + Vnz ($P \leq 0.05$) groups, when compared with control one (*Fig. 5A'*). In contrast, DHT or Vnz administration led to an increased SIRT1 protein (*Fig. 5A'*) ($P \leq 0.01$; $P \leq 0.001$, respectively) expression in comparison with control cultures. Quite opposite situation was observed in the case of SIRT6. In granulosal cultures with the addition of T + Vnz or DHT + Vnz, expression level of SIRT6 was significantly higher ($P \leq 0.01$) in comparison to control cultures. Interestingly, Vnz upregulated ($P \leq 0.001$) SIRT6 expression (*Fig. 6B'*). Analyses of SIRT1 and SIRT6 concentration in cell lysates

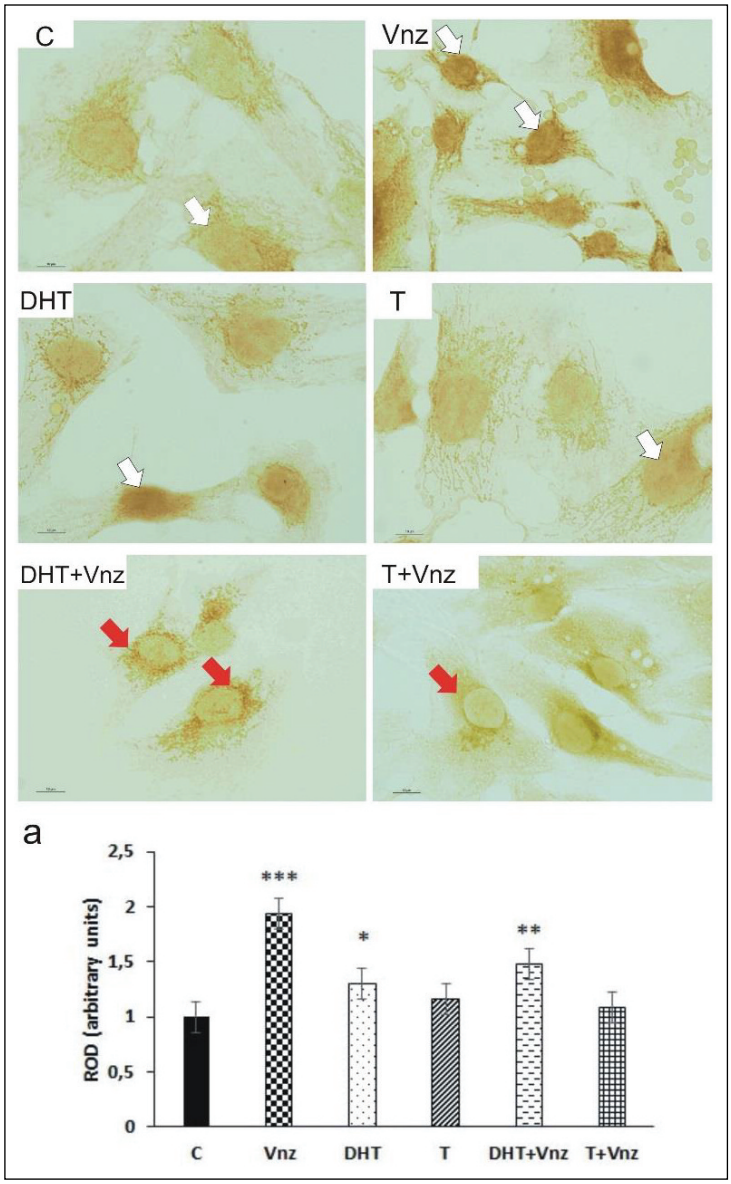

Fig. 1. Immunocytochemical localization of SIRT1 in porcine granulosa cell cultures. (C) Control cultures, (Vnz) cultures under vinclozolin influence, (DHT) cultures under dihydrotestosterone influence, (T) cultures under testosterone influence, (DHT + Vnz) cultures under DHT + Vnz influence, and (T + Vnz) cultures under T + Vnz influence. White arrows: nuclear/perinuclear localization of SIRT1 in granulosa cells. Red arrows: cytoplasmic and perinuclear staining of SIRT1 in granulosa cells. (a) The intensity of SIRT1 staining expressed as the relative optical density of the diaminobenzidine brown reaction products in granulosa cell cultures exposed to androgen receptor agonists (T and DHT), antagonist (Vnz), or both (T + Vnz and DHT + Vnz) versus respective controls. Values are mean ± standard error of the mean. Asterisks indicate significant differences between control and experimental cultures. Significant differences from control values are denoted as *$P \leq 0.05$, **$P \leq 0.01$ and ***$P \leq 0.001$, and were determined by Tukey's test. Bars: 10 µm.

performed by ELISA assays confirmed data obtained from Western blot (*Fig. 7*). In addition, SIRT1 deacetylase activity was higher in both DHT- and Vnz-treated GCs compared with control cultures (*Fig. 8*).

In follicular cultures significant ($P \leq 0.001$) SIRT1 protein upregulation was observed only after Vnz treatment. Similarly, addition of Vnz to the follicular culture caused significant increase in ($P \leq 0.001$) SIRT6 protein expression.

The effect of vinclozolin on granulosal and follicular sirtuins mRNA expression

We applied RT-PCR analysis to quantitatively evaluate SIRT1 and -6 mRNA expression in GCs lysates and follicular homogenates. Expression of both sirtuins mRNA was detected in both granulosal and follicular control cultures and those stimulated by AR agonists, the environmental AR antagonist, and combinations of both. The expression of sirtuins mRNA was normalized to GAPDH mRNA and presented as the 2-ΔCt. Relative sirtuins transcript levels in samples of experimental GCs and follicles were compared with those of the control.

As shown in *Fig. 5A* and *5B*, gene expression analysis revealed statistically significant changes in SIRT1 and SIRT6 mRNA levels in GCs cultured with the addition of DHT, Vnz, and DHT + Vnz. In these samples, SIRT1 transcript levels were statistically higher, whereas no differences were found within groups treated with T and T + Vnz. Gene expression analysis revealed statistically significant increases in SIRT6 mRNA levels

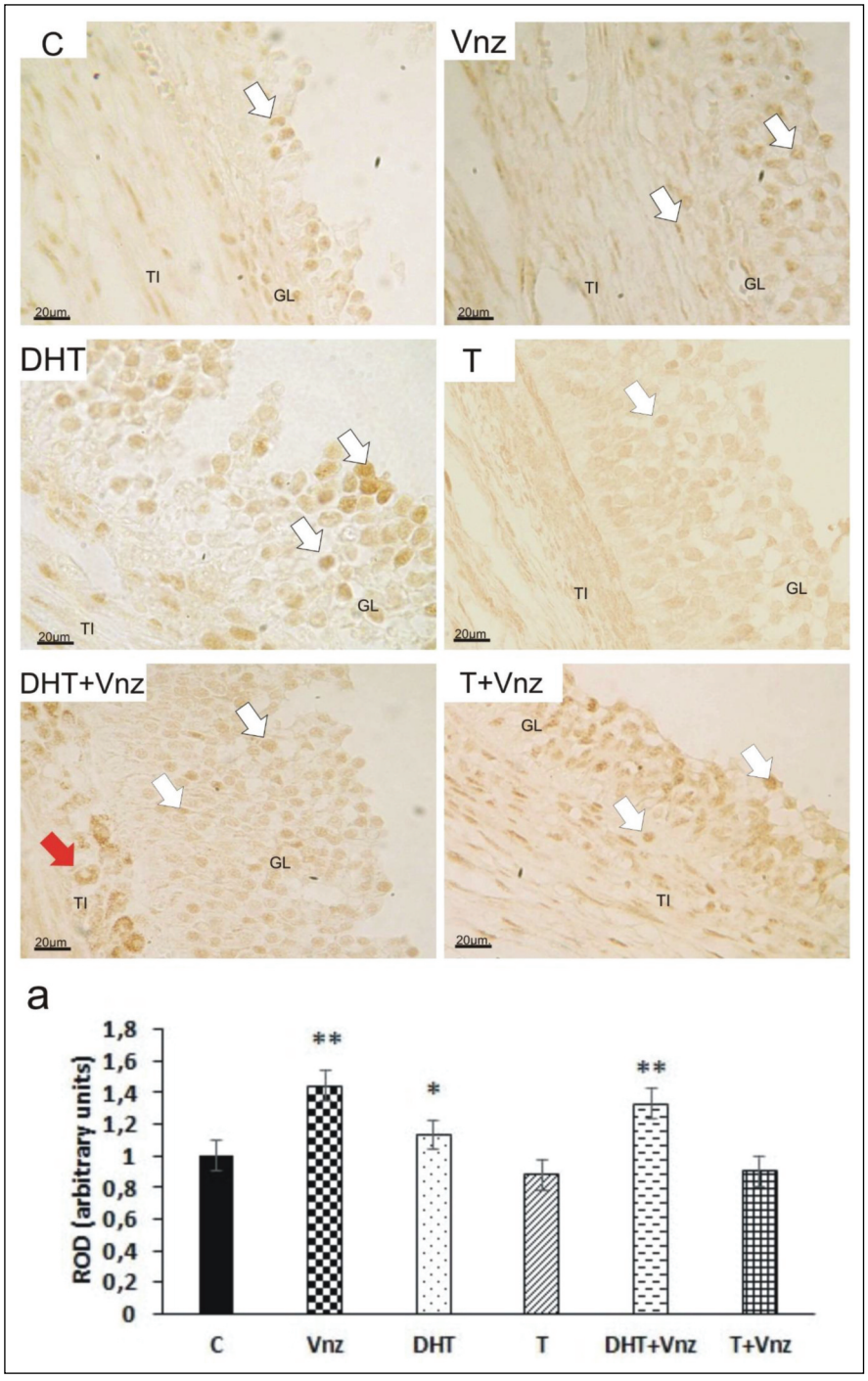

Fig. 2. Immunohistochemical localization of SIRT1 in cultured porcine ovarian follicles. (C) Control cultures, (Vnz) cultures under vinclozolin influence, (DHT) cultures under dihydrotestosterone influence, (T) cultures under testosterone influence, (DHT + Vnz) cultures under DHT + Vnz influence, and (T + Vnz) cultures under T + Vnz influence. White arrows: nuclear/perinuclear localization of SIRT1 in granulosa layer (GL) and theca interna cells (TI). Red arrows: cytoplasmic and perinuclear staining of SIRT1 in TI. (a) The intensity of SIRT1 staining expressed as the relative optical density of the diaminobenzidine brown reaction products in granulosa cell cultures exposed to androgen receptor agonists (T and DHT), antagonist (Vnz), or both (T + Vnz and DHT + Vnz) versus respective controls. Values are mean ± standard error of the mean. Asterisks indicate significant differences between control and experimental cultures. Significant differences from control values are denoted as $*P \leq 0.05$ and $**P \leq 0.01$, and were determined by Tukey's test. Bars: 20 µm.

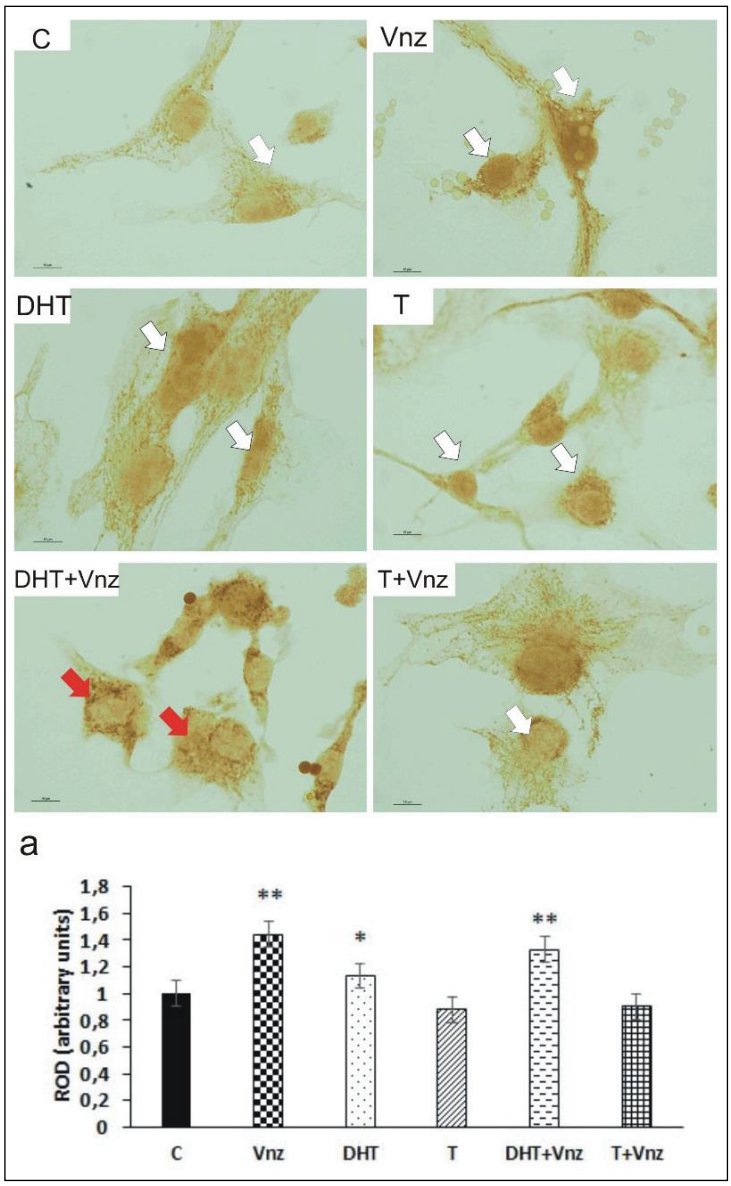

Fig. 3. Immunocytochemical localization of SIRT6 in porcine granulosa cell cultures. (C) Control cultures, (Vnz) cultures under vinclozolin influence, (DHT) cultures under dihydrotestosterone influence, (T) cultures under testosterone influence, (DHT + Vnz) cultures under DHT + Vnz influence, and (T + Vnz) cultures under T + Vnz influence. White arrows: nuclear/perinuclear localization of SIRT6 in granulosa cells. Red arrows: cytoplasmic and perinuclear staining of SIRT1 in granulosa cells. (a) The intensity of SIRT6 staining expressed as the relative optical density of the diaminobenzidine brown reaction products in granulosa cell cultures exposed to androgen receptor agonists (T and DHT), antagonist (Vnz), or both (T + Vnz and DHT + Vnz) versus respective controls. Values are mean ± standard error of the mean. Asterisks indicate significant differences between control and experimental cultures. Significant differences from control values are denoted as *P ≤ 0.05 and **P ≤ 0.01, and were determined by Tukey's test. Bars: 10 µm.

in GCs cultured with Vnz (P ≤ 0.01) and DHT + Vnz (P ≤ 0.05). The significant decrease in SIRT6 mRNA transcript level was observed in cells treated with T (*Fig. 5A*).

Quite the opposite situation was observed concerning follicular SIRT1 mRNA expression; only T or T + Vnz increased SIRT1 mRNA expression (P ≤ 0.05 and P ≤ 0.01, respectively) as compared with that of the control group (*Fig. 6B*).

DISCUSSION

Results of many studies in the area of reproductive toxicity indicate harmful effects of EDCs present in the environment (49). Therefore understanding both the target and mechanisms of their action as well as the elaboration of prevention strategies are constantly needed (50). Among EDCs there is a large group of chemicals exerting antiandrogenic effects and blocking endogenous androgens action. We can find there environmental contaminants: pesticides *e.g.* vinclozolin (51). During our previous experiments concerning the involvement of androgens in ovarian follicular development and atresia we generated an *in vitro* toxicological model for studying results of androgen deficiency. Using 2-hydroxyflutamide, which is a nonsteroidal anti-androgen acting at the AR level, we induced distortions of androgen action in the porcine ovary what in consequence reduced GCs viability and proliferation (52). Next, we have shown that vinclozolin at an environmentally-relevant concentration might contribute to the amplification and propagation of apoptotic cell death in the granulosa layer, leading to the rapid removal of atretic follicles in the porcine ovary. Besides, it seems possible that vinclozolin activates non-genomic signaling pathways directly modifying the androgen receptors action (27, 33).

Androgens play a pivotal role in mammalian follicle development, but still little data is available regarding the connection between androgens and sirtuins expression in follicular cells. The current research for the first time shows that experimentally induced androgen deficiency during porcine granulosal and follicular *in vitro* culture significantly changes SIRT1 and SIRT6 mRNA and protein expression what may have deleterious effects on follicular survivability and function. It was found out that Vnz alone or in combination with androgens acted directly on the expression of the investigated sirtuin genes and proteins. In line with multiple studies confirming that in the

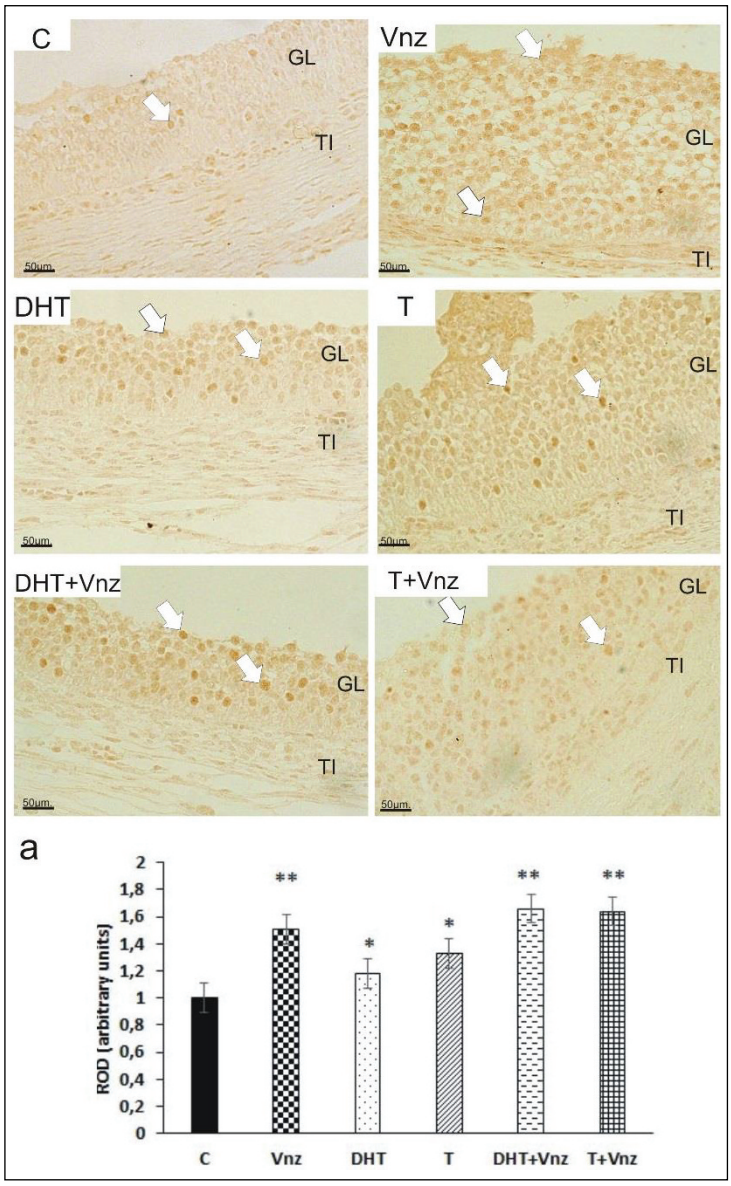

Fig. 4. Immunohistochemical localization of SIRT6 in cultured porcine ovarian follicles. (C) Control cultures, (Vnz) cultures under vinclozolin influence, (DHT) cultures under dihydrotestosterone influence, (T) cultures under testosterone influence, (DHT + Vnz) cultures under DHT + Vnz influence, and (T + Vnz) cultures under T + Vnz influence. White arrows: nuclear/perinuclear localization of SIRT6 in granulosa layer (GL) and theca interna cells (TI). (a) The intensity of SIRT6 staining expressed as the relative optical density of the diaminobenzidine brown reaction products in granulosa cell cultures exposed to androgen receptor agonists (T and DHT), antagonist (Vnz), or both (T + Vnz and DHT + Vnz) versus respective controls. Values are mean ± standard error of the mean. Asterisks indicate significant differences between control and experimental cultures. Significant differences from control values are denoted as *P ≤ 0.05, **P ≤ 0.01, and were determined by Tukey's test. Bars: 50 µm.

ovary various proteins are targets of endocrine disruptors (53), our results clearly indicate that Vnz, possibly acting *via* ARs and/or by non-genomic mechanisms, has influence on the investigated sirtuins in porcine ovarian follicular cells.

Sirtuins, which play important roles *i.e.* in the regulation of metabolism, reproductive physiology, aging or oncogenesis (54), are recently perceived as emerging factors in the regulation of steroid hormone receptor signaling (55). They can regulate steroid hormone signaling through a variety of molecular mechanisms, including: operation as co-regulatory transcription factors, deacetylation of histones in the promoters of genes with nuclear receptor-binding sites, direct deacetylation of steroid hormone nuclear receptors, and regulation of pathways that modify steroid hormone receptors through phosphorylation (56).

It has been reported that SIRT1 was expressed in rat and pig ovarian tissue (10, 13) and human luteinized GCs (57). The present study confirmed previous findings that SIRT1 is widely expressed in the porcine ovarian follicle, especially in GCs, theca cells and oocytes (13-15). In GCs exposed to Vnz, expression of SIRT1 protein showed the most prominent increase suggesting its association with impaired cell survival qualities under this fungicide influence. Moreover, the level of SIRT1 protein expression in follicles treated with Vnz was remarkably elevated, what was in compliance with their low development potential as we have shown previously (33). Our findings are consistent with results obtained by Zhao *et al.* (13). They demonstrated, that SIRT1 expression was weak in the GCs of healthy follicles, but its high level have occurred in early atretic ones what indicates that SIRT1 may be involved in GCs apoptosis during follicular atresia in pig.

SIRT1 regulates cell biology, metabolism, and fate at different levels through the deacetylation of histones and other cellular factors such as p53 or nuclear factor-kappa B (NF-κB). Previous studies have demonstrated that in rats kept under caloric restriction, an increased endogenous SIRT1 level downregulates the expression of p53, reduces follicle atresia, and maintains the ovarian reserve (58). Zhou *et al.* (59) have demonstrated that treatment with SIRT1 activator (SRT1720) may promote the ovarian lifespan of high-fat diet-induced obese female mice by suppressing the activation of primordial follicles, follicle maturation, and atresia *via* the activation of SIRT1 signaling and suppression of mTOR signaling. On the

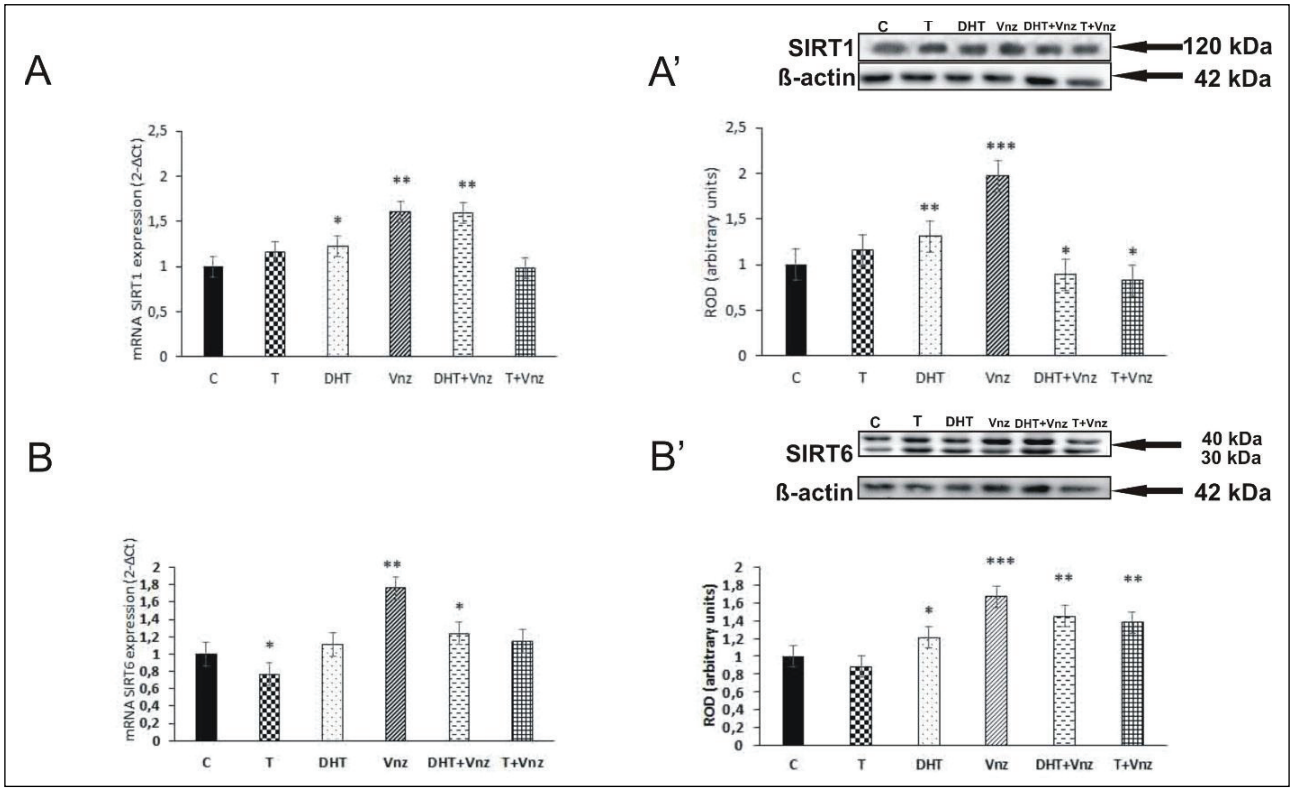

Fig. 5. Expression of mRNA and protein for SIRT1 (A, A') and SITR6 (B, B') in cultured porcine granulosa cells. Relative expression of mRNAs for SIRT1 (A) and SIRT6 (B) was determined using quantitative real-time polymerase chain reaction (PCR) analysis. Relative quantification (RQ) is expressed as mean ± SEM. Asterisks indicate statistically significant differences (*P ≤ 0.05, **P ≤ 0.01; Tukey's *post hoc* test). Representative blots of Western blot analysis and relative expression of SIRT1 (A') and SIRT6 (B') are shown. Semiquantitative densitometric analysis of proteins content were normalized against its corresponding β-actin data point. The proteins level within the control group was arbitrarily set as 1. Data obtained from three separate experiments are expressed as mean ± SEM. Asterisks indicate statistically significant differences (* P ≤ 0.05,** P ≤ 0.01; *** P ≤ 0.001; Tukey's *post hoc* test). *Abbreviations:* C, Control cultures; T, cultures under testosterone influence; DHT, cultures under dihydrotestosterone influence; Vnz, cultures under vinclozolin influence; DHT + Vnz, cultures under DHT + Vnz influence; T + Vnz, cultures under T + Vnz influence.

contrary to the aforementioned results, in our previous studies we have shown the significant increase in p53 protein level in porcine GCs after Vnz and Vnz + DHT treatment (33). Together with the stimulation of SIRT1 after fungicide exposure observed during our current study, we can speculate that Vnz upregulates SIRT1 expression causing overexpression of p53 what accelerates apoptosis of GCs. Based on this and results obtained by Sirotkin *et al.* (15) also conducted on the porcine GCs *in vitro* model, the existence of a stimulatory influence of SIRT1 on apoptosis in ovarian follicular cells can be proposed.

Kuo *et al.* (60) have demonstrated that SIRT1 inhibits breast cancer progression. It was shown that SIRT1 downregulates the expression of a pro-survival Bcl-2 protein in cultured human breast cancer cells. As we reported previously (33), expression of Bcl-2 was significantly lower in GCs cultured under Vnz influence. Therefore, it seems possible that upregulation of SIRT1 caused by this fungicide action, directly influences expression of the anti-apoptotic protein Bcl-2. In accordance to the above-cited data, the outcomes from Zhao *et al.* (13) study strongly support the role of SIRT1 during the process of follicular atresia. Based on this and our findings we might suggest that in the porcine ovary the augmentation of SIRT1 expression may be related to follicular failure.

The relationship between cell proliferation and differentiation is fundamental to all biological processes. Nonproliferating and nondifferentiating cells are usually excluded from apoptosis. Cells exposed to strong proapoptotic factors start NF-κB pathway with secretion of TNF-α and expression of TNFR1 (61). Vnz granulosal treatment caused high expression of TNF-α and as a consequence, high activation levels of TNFR1 (33). Together with high level of SIRT1 reported here it has become apparent that Vnz-induced intense SIRT1 signaling and activation of NFκB signaling what may be a causative factor in the decline of GCs viability. SIRT1 can directly reduce GCs viability, but on the other hand, recent data by Pavlova *et al.* (14) have revealed that overexpression of SIRT1 by transfection in porcine GCs leads to the accumulation of proliferation markers such as cyclin B1. Thus, it seems possible that granulosa cell fate depends on the ovarian cell state and balance between inhibitory and stimulatory influences on SIRT1 (15). Interestingly, there are several papers suggesting that a decline in SIRT1 expression in the ovarian tissue may be a cause of disturbances in female reproductive functions. Tao *et al.* (62) using the experimental model of polycystic ovary syndrom (PCOS) rats, concluded that a significant decrease in the expression of SIRT1 in ovarian tissue may be directly involved in the development and progression of PCOS. Furat Rencber *et al.* (63) found that activation of SIRT1 can improve weight gain, hormone profile and ovarian follicular cell structure in PCOS rats. Research conducted on human ovaries (64), however, suggest that SIRT1 can function as an anti-apoptotic factor in granular ovarian cells by regulating the ERK1/2

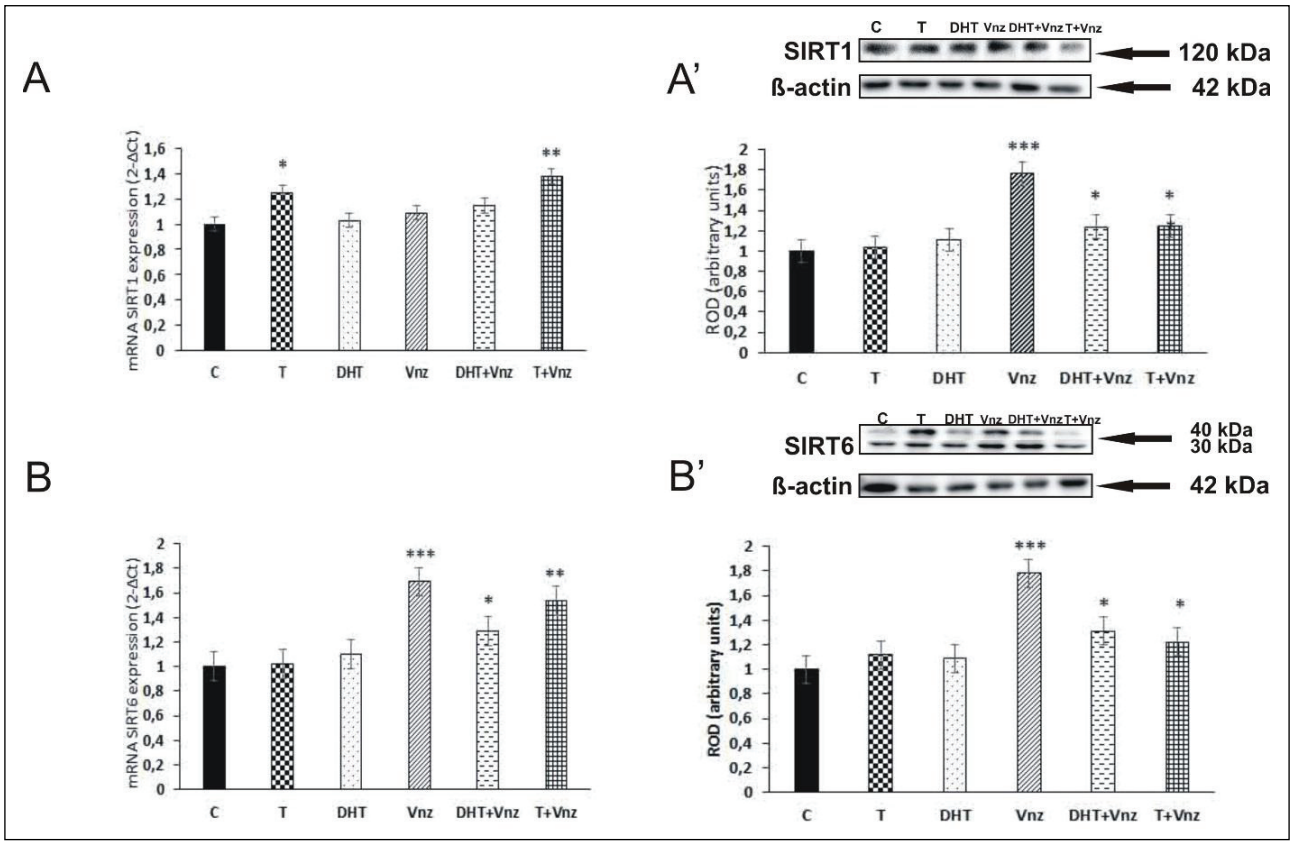

Fig. 6. Expression of mRNA and protein for SIRT1 (A, A') and SITR6 (B, B') in cultured porcine follicles. Relative expression of mRNAs for SIRT1 (A) and SIRT6 (B) was determined using quantitative real-time polymerase chain reaction (PCR) analysis. Relative quantification (RQ) is expressed as mean ± SEM. Asterisks indicate statistically significant differences (* $P \leq 0.05$, ** $P \leq 0.01$, *** $P \leq 0.001$; Tukey's *post hoc* test). Representative blots of Western blot analysis and relative expression of SIRT1 (A') and SIRT6 (B') are shown. Semiquantitative densitometric analysis of proteins content were normalized against its corresponding β-actin data point. The proteins level within the control group was arbitrarily set as 1. Data obtained from three separate experiments are expressed as mean ± SEM. Asterisks indicate statistically significant differences (* $P \leq 0.05$; *** $P \leq 0.001$; Tukey's *post hoc* test). C, Control cultures; T, cultures under testosterone influence; DHT, cultures under dihydrotestosterone influence; Vnz, cultures under vinclozolin influence; DHT + Vnz, cultures under DHT + Vnz influence; T+ Vnz, cultures under T + Vnz influence.

pathway. In other words, as reported by Coussens *et al.* (65), the mechanism of SIRT1 action is pleiotropic and dependent on cell type and/or stage of development, and on the species tested.

In this study we provided the evidence that the lesser known SIRT6 might be also a key factor for proper ovarian function. Recent studies have established that SIRT6 is involved in genomic DNA stability and repair and is possibly linked to cellular metabolism and aging. Through specific histone H3 lysine 56 (H3K56) deacetylase activity, SIRT6 is able to participate in the regulation of DNA stabilization and repair (66, 67). In addition, SIRT6 has been found to interact with NF-κB and to deacetylate histone H3 lysine 9 (H3K9) at NF-κB target gene promoters, leading to the inactivation of many of the transcription factors characteristic of aged tissues (68). It has been also shown that SIRT1 and SIRT6 may be involved in the mechanism by which caloric restriction inhibits the transition from primordial to developing follicles, extends the entire growth phase of a follicle to preserve the reserve of germ cells, and delays age-related ovarian aging (9). Overall, these findings suggest that SIRT6 next to SIRT1 are key members of the sirtuin family that exert a wide range of actions in the regulation of cellular physiology and aging. Here we demonstrated the expression of SIRT6 in porcine granulosal and follicular cells by immunocyto/immunohistochemical and Western blot analysis, and the expression of its mRNA by RT-PCR. To our knowledge, this is the first report that SIRT6 is expressed in the porcine ovarian follicular cells. Expression of SIRT6 was observed mainly in the nuclei of granulosa cells. It is worth mentioning that Vnz treatment caused an increase in SIRT6 mRNA and protein levels. Our study suggests that overexpression of SIRT6 may remarkably promote apoptosis of GCs, which is in agreement with results obtained by Van Metter *et al.* (69). They have shown that SIRT6 remarkably promotes apoptosis in a variety of cancer cells, which requires the activation of p53 apoptotic signaling cascades. However, the precise role of SIRT6 in the porcine ovary is still poorly known and needs further exploration.

Taken together, our study provides evidence that SIRT1 and SIRT6 are present in the porcine ovarian follicles. We demonstrated that in response to Vnz stimulus in follicular and granulosal cultures the level of both investigated sirtuins remarkably increased. Taking into account this and our previous results we suppose that the deleterious effects in the ovarian follicles after fungicide exposure might be directly related to the overexpression of SIRT1 and SIRT6. Understanding the mechanism of action of the investigated sirtuins on the function of granulosal and follicular cells, their receptors, secreted steroid hormones and production of other non-hormonal molecules needs further intensive studies and highly advanced research tools.

Authors' contribution: GG, KW, MD performed the research; MD analyzed the data; ZT critically read and revised

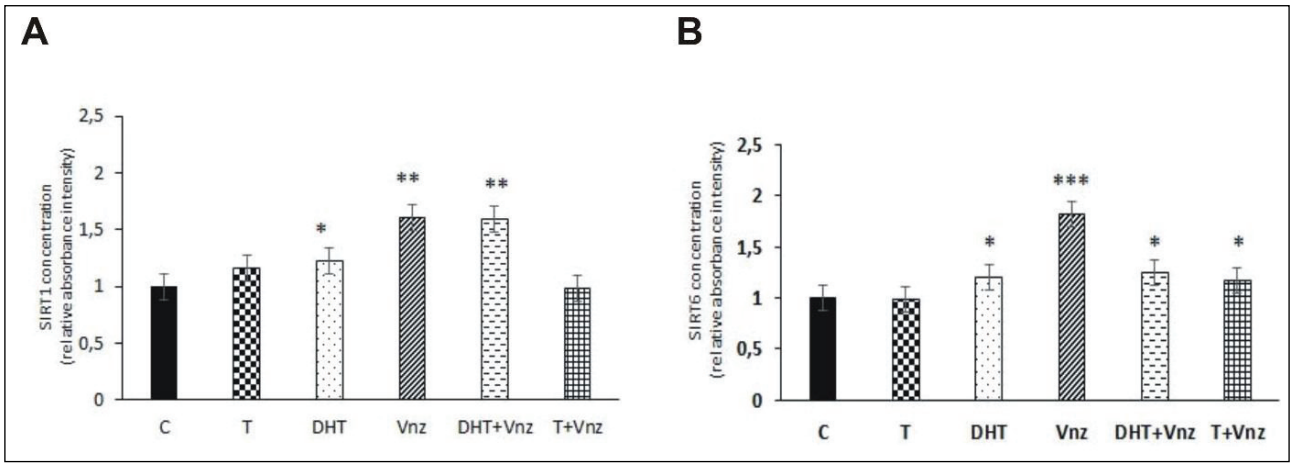

Fig. 7. Effects of vinclozolin (Vnz) on SIRT1 (A) and SIRT6 (B) concentration in granulosa cells after treatment with testosterone (T), dihydrotestosterone (DHT), vinclozolin (Vnz), T + Vnz, or DHT + Vnz. Values are expressed as mean ± standard error of the mean (n = 3). Significant differences from control values are denoted as *P ≤ 0.05, **P ≤ 0.01, and ***P ≤ 0.001 and were determined by Tukey's *post hoc* test.

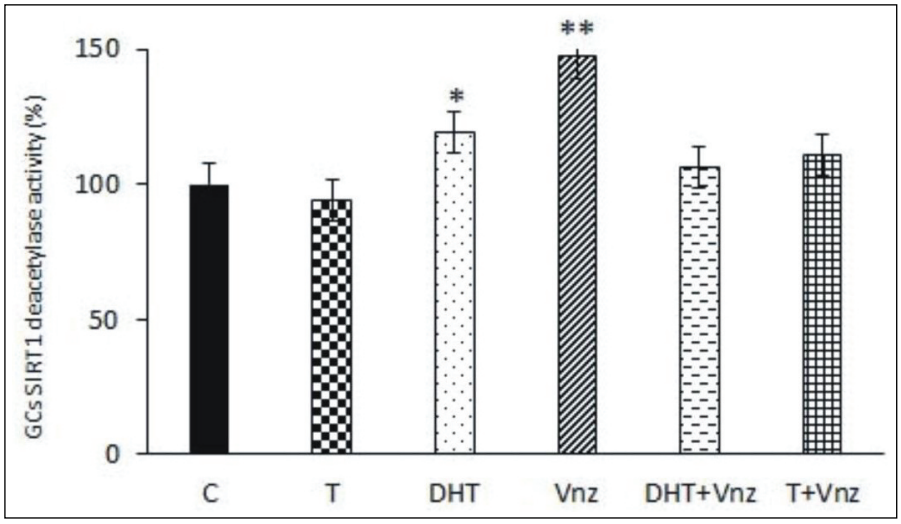

Fig. 8. The SIRT1 deacetylase activity in cultured porcine follicles is expressed as percent relative to Control cultures of GCs. Values are expressed as mean ± standard error of the mean (n = 3). Significant differences from control values are denoted as **P ≤ 0.01 and were determined by Tukey's *post hoc* test. (C) Control cultures, (T) cultures under testosterone influence, (DHT) cultures under dihydrotestosterone influence, (Vnz) cultures under vinclozolin influence, cultures under DHT + Vnz influence, and cultures under T + Vnz influence.

the manuscript; MD designed the research study and wrote the paper with ZT contribution. All authors have read and approved the final version of the manuscript.

Acknowledgments: The authors are very grateful to Ms. Beata Snakowska (Department of Endocrinology, Institute of Zoology and Biomedical Research, Jagiellonian University) for technical assistance. This work was supported by DEC-2013/09/B/NZ9/00226 from National Science Centre Poland and Faculty of Biology grant K/DSC/005534.

Conflict of interests: None declared.

REFERENCES

1. Schwer B, Verdh E. Conserved metabolic functions of sirtuins. *Cell Metab* 2008; 7: 104-112.
2. Haigis MC, Guarente LP. Mammalian sirtuins-emerging roles in physiology, aging and calorie restriction. *Genes Dev* 2006; 20: 2913-2921.
3. Finkel T, Deng CX, Mostoslavsky R. Recent progress in the biology and physiology of sirtuins. *Nature* 2009; 460: 587-591.
4. Pardo PS, Mohamed JS, Lopez MA, Boriek AM. Introduction of Sirt1 by mechanical stretch of skeletal muscle through the early response factor EGR1 triggers an antioxidative response. *J Biol Chem* 2011; 286: 2559-2566.
5. Bell EL, Emerling BM, Ricoult SJ, Guarente L. Sirt3 suppresses hypoxia inducible factor1 alpha and tumor growth by inhibiting mitochondrial ROS production. *Oncogene* 2011; 30: 2986-2996.
6. Ahn BH, Kin H, Song S, *et al.* A role for mitochondrial deacetylase Sirt3 in regulatory energy homeostasis. *Proc Natl Acad Sci USA* 2008; 105: 14447-14452.
7. Picard F, Kurtev M, Chung N, *et al.* Sirt1 promotes fat mobilization in white adipocytes by repressing PPAR-γ. *Nature* 2004; 429: 771. doi: 10.1038/nature02583
8. Al-Hakeim HK, Jebur IM, Rahim AI. SIRT6 is correlated with estradiol in women with in vitro fertilization failure. *Int J Pharm Pharm Sci* 2016; 8: 184-188.
9. Luo L, Chen XC, Fu YC, *et al.* The effects of caloric restriction and a high-fat diet on ovarian lifespan and the

expression of SIRT1 and SIRT6 proteins in rats. *Aging Clin Exp Res* 2012; 24: 125-133.
10. Morita Y, Wada-Hiraike O, Yano T, *et al.* Resveratrol promotes expression of SIRT1 and StAR in rat ovarian granulosa cells: an implicative role of SIRT1 in the ovary. *Reprod Biol Endocrinol* 2012; 10: 14. 10.1186/1477-7827-10-14
11. Di Emidio G, Falone S, Vitti M, *et al.* SIRT1 signalling protects mouse oocytes against oxidative stress and is deregulated during aging. *Hum Reprod* 2014; 29: 2006-2017.
12. Long GY, Yang JY, Xu JJ, *et al.* SIRT1 knock-in mice preserve ovarian reserve resembling caloric restriction. *Gene* 2019; 20: 194-202.
13. Zhao F, Zhao W, Ren S, *et al.* Roles of SIRT1 in granulosa cell apoptosis during the process of follicular atresia in porcine ovary. *Anim Reprod Sci* 2014; 151: 34-41.
14. Pavlova S, Klucska K, Vasicek D, *et al.* The involvement of SIRT1 and transcription factor NF-κB (p50/p65) in regulation of porcine ovarian cell function. *Anim Reprod Sci* 2013; 40: 180-188.
15. Sirotkin AV, Dekanova P, Harrath AH, Alwasel SH, Vasicek D. Interrelationships between sirtuin 1 and transcription factors p53 and NF-□B (p50/p65) in the control of ovarian cell apoptosis and proliferation. *Cell Tissue Res* 2014; 358: 627-632.
16. Jakimiuk AJ, Nowicka MA, Zagozda M, Koziol A, Lewandowski P, Issat T. Hogh level of soluble vascular endothelial growth factor receptor 1/SFLT1 and low levels of vascular endothelial growth factor in follicular fluid on the day of oocyte retrieval correlate with ovarian hyperstimulation syndrome regardless of the stimulation protocol. *J Physiol Pharmacol* 2017; 68: 477-484.
17. Nagyova E, Nemcowa L, Bujnakowa-Mlynarcikowa A, Blaha M, Prohazka R, Scsukova S. Effect of bone morphogenetic protein-15 on gonadotropin - stimulated synthesis of hyaluronan and progesterone in porcine ovarian follicle. *J Physiol Pharmacol* 2017; 68: 683-691.
18. Lebbe M, Woodruff TK. Involvement of androgens in ovarian health and disease. *Mol Hum Reprod* 2013; 19: 828-837.
19. Gervasio CG, Bernuci MP, Silva-de-Sa MF, Rosa-e-Silva AC. The role of androgen hormones in early follicular development. *ISRN Obstet Gynecol* 2014; 2014: 818010. doi: 10.1155/2014/818010
20. Prizant H, Gleicher N, Sen A. Androgen action in the ovary: balance is key. *J Endocrinol* 2014; 222: R141-R151.
21. Walters KA, Allan CM, Handelsman DJ. Androgen actions and the ovary. *Biol Reprod* 2008; 78: 380-389.
22. Salvetti NR, Ortega HH, Veiga-Lopez A, Padmanabhan V. Developmental programming: impact of prenatal testosterone excess on ovarian cell proliferation and apoptotic factors in sheep. *Biol Reprod* 2012; 87: 22. doi: 10.1095/biolreprod.112.100024
23. Veiga-Lopez A, Ye W, Padmanabhan V. Developmental programming: prenatal testosterone excess disrupts anti-Mullerian hormone expression in preantral and antral follicles. *Fertil Steril* 2012; 97: 748-756.
24. Duda M, Durlej-Grzesiak M, Tabarowski Z, Slomczynska M. Effects of testosterone and 2-hydroxyflutamide on progesterone receptor expression in porcine ovarian follicles in vitro. *Reprod Biol* 2012; 12: 333-340.
25. Durlej M, Knapczyk-Stwora K, Duda M, *et al.* Prenatal and neonatal exposure to the antiandrogen flutamide alters connexin 43 gene expression in adult porcine ovary. *Domest Anim Endocrinol* 2011; 40: 19-29.
26. Duda M, Grzesiak M, Knet M, *et al.* The impact of antiandrogen 2-hydroxyflutamide on the expression of steroidogenic enzymes in cultured porcine ovarian follicles. *Mol Biol Rep* 2014; 41: 4213-4222.
27. Knet M, Tabarowski Z, Slomczynska M, Duda M. The effects of the environmental antiandrogen vinclozolin on the induction of granulosa cell apoptosis during follicular atresia in pigs. *Theriogenology* 2014; 81: 1239-1247.
28. van Ravenzwaay B, Kolle SN, Ramirez T, Kamp HG. Vinclozolin: a case study on the identification of endocrine active substance in the past and a future perspective. *Toxicol Lett* 2013; 223: 271-279.
29. Kavlock R, Cummings A. Mode of action: inhibition of androgen receptor function-vinclozolin-induced malformations in reproductive development. *Crit Rev Toxicol* 2005; 35: 721-726.
30. Kiparissis Y, Metcafle TL, Balch GC, Metcalfe CD. Effects of the antiandrogens, vinclozolin and cyproterone acetate on gonadal development in the Japanese medaka (Oryzias latipes). *Aquat Toxicol* 2003; 63: 391-403.
31. Nilsson EE, Anway MD, Stanfield J, Skinner MK. Transgenerational epigenetic effects of the endocrine disruptor vinclozolin on pregnancies and female adult onset disease. *Reproduction* 2008; 135: 713-721.
32. Buckley J, Willingham E, Agras K, Baskin LS. Embryonic exposure to the fungicide vinclozolin causes virilization of females and alteration of progesterone receptor expression in vivo: an experimental study in mice. *Environ Health* 2006; 5: 4. doi: 10.1186/1476-069X-5-4
33. Knet M, Wartalski K, Hoja-Lukowicz D, Tabarowski Z, Slomczynska M, Duda M. Analysis of porcine granulosa cell death signaling pathways induced by vinclozolin. *Theriogenology* 2015; 84: 927-939.
34. Wartalski K, Knet-Seweryn M, Hoja-Lukowicz D, Tabarowski Z, Duda M. Androgen receptor-mediated non-genomic effects of vinclozolin on porcine ovarian follicles and isolated granulosa cells: vinclozolin and non-genomic effects in porcine ovarian follicles. *Acta Histochem* 2016; 118: 377-386.
35. Dai Y, Ngo D, Forman LW, Qin DC, Jacob J, Faller DV. Sirtuin 1 is required for antagonist-induced transcriptional repression of androgen-responsive genes by the androgen receptor. *Mol Endocrnol* 2007; 21: 1807-1821.
36. Fu MF, Wang C, Reutens AT, *et al.* p300 and p300/cAMP response element-binding protein-associated factor acetylate the androgen receptor at sites governing hormone-dependent transactivation. *J Biol Chem* 2000; 275: 20853-20860.
37. Fu M, Liu M, Sauve AA, *et al.* Hormonal control of androgen receptor function through SIRT1. *Mol Cell Biol* 2006; 26: 8122-8135.
38. Lin P, Rui R. Effects of follicular size and FSH on granulosa cell apoptosis and atresia in porcine antral follicles. *Mol Reprod Dev* 2010; 77: 670-678.
39. Gregoraszczuk EL, Skalka M. Thyroid hormone as a regulator of basal and human chorionic gonadotropin - stimulated steroidogenesis by cultured porcine theca and granulosa cells isolated at different stages of the follicular phase. *Reprod Fertil Dev* 1996; 8: 961-967.
40. Stoklosowa S. Tissue culture of gonadal cells. *Acta Biol Acad Sci Hung* 1982; 33: 367-379.
41. Gregoraszczuk E. Steroid hormone release in cultures of pig corpus luteum and granulosa cells. *Endocrinol Exp* 1983; 17: 59-68.
42. Conley A, Hinshelwood M. Mammalian aromatases. *Reproduction* 2001; 121: 685-695.
43. Weihua Z, Lathe R, Warner M, Gustafsson JA. An endocrine pathway in the prostate, ER-beta, AR, 5alpha-androstane-3beta,17beta-diol, and CYP7B1, regulates prostate growth. *Proc Natl Acad Sci USA* 2002; 99: 13589-13594.
44. Shikanov A, Xu M, Woodruff TK, Shea LD. A method of ovarian follicle encapsulation and culture in proteolytically

degradable 3 dimensional system. *J Vis Exp* 2011; (49): 2695. doi: 10.3791/2695
45. Smolen AJ. Image analytic techniques for quantification of immunocytochemical staining in the nervous system. In: Methods in Neurosciences, Conn PM (ed.), New York, Academic Press 1990, pp. 208-229.
46. Laemmli UK. Cleavage of structural proteins during the assembly of the head of bacteriophage T4. *Nature* 1970; 227: 680-685.
47. Grzesiak M, Knapczyk-Stwora K, Slomczynska M. induction of autophagy in the porcine corpus luteum of pregnancy following anti-androgen treatment. *J Physiol Pharmacol* 2016; 67: 933-942.
48. Livak KJ, Schmittgen TD. Analysis of relative gene expression data using real-time quantitative PCR and the 2-ΔΔCt method. *Methods* 2001; 25: 402-408.
49. Wang A, Padula A, Sirota M, Woodruff TJ. Environmental influences on reproductive health, the importance of chemical exposures. *Fertil Steril* 2016; 106: 905-929.
50. Inhorn MC, Patrizio P. Infertility around the globe: new thinking on gender, reproductive technologies and global movements in the 21st century. *Hum Reprod Update* 2015; 21: 411-426.
51. Hejmej A, Kotula-Balak M, Bilinska B. Antiandrogenic and estrogenic compounds: effect on development and function of male reproductive system. In: Steroids - Clinical Aspect, Abduljabbar H. (ed.), InTech 2011, pp. 51-82.
52. Duda M, Durlej M, Knet M, Knapczyk-Stwora K, Tabarowski Z, Slomczynska M. Does 2-hydroxyflutamide inhibit apoptosis in porcine granulosa cells? - an in vitro study. *J Reprod Dev* 2012; 58: 438-444.
53. Patel S, Zhou C, Rattan S, Flaws JA. Effects of endocrine-disrupting chemicals on the ovary. *Biol Reprod* 2015; 93: 20. doi: 10.1095/biolreprod.115.130336
54. Tatone C, Di Emidio G, Barbonetti A, *et al.* Sirtuins in gamete biology and reproductive physiology: emerging roles and therapeutic potential in female and male infertility. *Hum Rep Update* 2018; 24: 267-289.
55. Gronemeyer H, Gustafsson JA, Laudet V. Principles for modulation of the nuclear receptor superfamily. *Nat Rev Drug Discov* 2004; 3: 950-964.
56. Huang PX, Chandra V, Rastinejad F. Structural overview of the nuclear receptor superfamily: insights into physiology and therapeutics. *Annu Rev Physiol* 2010; 72: 247-272.
57. Benayoun BA, Georges AB, L'Hote D, *et al.* Transcription factor FOXl2 protects granulosa cells from stress and delays cell cycle: role of its regulation by the SIRT1 deacetylase. *Hum Mol Genet* 2011; 20:1673-1686.
58. Xiang Y, Xu J, Li L, *et al.* Calorie restriction increases primordial follicle reserve in mature female chemotherapy-treated rats. *Gene* 2012; 493: 77-82.
59. Zhou XL, Xu JJ, Ni YH, *et al.* SIRT1 activator (SRT1720) improves the follicle reserve and prolongs ovarian lifespan of diet-induced obesity in female mice via activating SIRT1 and suppressing mTOR signaling. *J Ovarian Res* 2014; 7: 97-107.
60. Kuo SJ, Lin HY, Chien SY, Chen DR. SIRT1 suppresses breast cancer growth through downregulation of the Bcl-2 protein. *Oncol Rep* 2013; 30: 125-130.
61. Biton S, Ashkenazi A. NEMO and RIP1 control cell fate in response to extensive DNA damage via TNF-alpha feedforward signaling. *Cell* 2011; 145: 92-103.
62. Tao X, Zhang X, Ge S, Zhang E, Zhang B. Expression of SIRT1 in the ovaries of rats with polycystic ovary syndrome before and after therapeutic intervention with exenatide. *Int J Clin Exp Pathol* 2015; 8: 8276-8283.
63. Furat Rencber S, Kurnaz Ozbek S, Eraldemır C, *et al.* Effect of resveratrol and metformin on ovarian reserve and ultrastructure in PCOS: an experimental study. *J Ovarian Res* 2018; 11: 55. doi: 10.1186/s13048-018-0427-7
64. Han Y, Luo H, Wang H, Cai J, Zhang Y. SIRT1 induces resistance to apoptosis in human granulosa cells by activating the ERK pathway and inhibiting NF-κB signaling with anti-inflammatory functions. *Apoptosis* 2017; 22: 1260-1272.
65. Coussens M, Maresh JG, Yanagimachi R, Maeda G, Allsopp R. Sirt1 deficiency attenuates spermatogenesis and germ cell function. *PLoS One* 2008; 3: e1571. doi: 10.1371/journal.pone.0001571
66. Michishita E, McCord RA, Berber E, *et al.* SIRT6 is a histone H3 lysine 9 deacetylase that modulates telomeric chromatin. *Nature* 2008; 452: 492-496.
67. Yang B, Zwaans BM, Eckersdorff M, Lombard DB. The sirtuin SIRT6 deacetylates H3 K56Ac in vivo to promote genomic stability. *Cell Cycle* 2009; 8: 2662-2663.
68. Kawahara TL, Michishita E, Adler AS, *et al.* SIRT6 links histone H3 lysine 9 deacetylation to NF-κB-dependent gene expression and organismal life span. *Cell* 2009; 136: 62-74.
69. Van Metter M, Mao Z, Gorbunowa V, Seluanov A. SIRT6 overexpression induces massive apoptosis in cancer cells but not in normal cells. *Cell Cycle* 2011; 10: 3153-3158.

Received: December 12, 2018
Accepted: February 28, 2019

Author's address: Dr. Malgorzata Duda, Department of Endocrinology, Institute of Zoology and Biomedical Research, Jagiellonian University, 9 Gronostajowa Street, 30-387 Cracow, Poland.
E-mail: maja.duda@uj.edu.pl